

ESA's X-RAY ASTRONOMY MISSION, XMM

B.G. TAYLOR and A. PEACOCK

Space Science Department, ESTEC-ESA, Noordwijk, The Netherlands

Abstract. ESA's X-ray Astronomy Mission, XMM, scheduled for launch in 1998, is the second of four cornerstones of ESA's long term science program Horizon 2000. Covering the range from about 0.1 to 10 keV, it will provide a high throughput of 5000 cm² at 7 keV with three independent telescopes, and have a spatial resolution better than 30 arcsec. Broadband spectrophotometry is provided by CCD cameras while reflection gratings provide medium resolution spectroscopy (resolving power of about 400) in the range 0.3–3 keV. Long uninterrupted observations will be made from the 24 hr period, highly eccentric orbit, reaching a sensitivity approaching 10⁻¹⁵ erg cm⁻² s⁻¹ in one orbit. A 30 cm UV/optical telescope is bore-sighted with the x-ray telescopes to provide simultaneous optical counterparts to the numerous serendipitous X-ray sources which will be detected during every observation.

1. Introduction

The concept of a high-throughput, medium spatial resolution, X-ray astronomy mission with spectroscopic capability over a wide energy band was studied extensively within ESA in the mid-80's.

A set of scientific requirements, in order of priority was established as outlined below.

1. Broad band spectroscopy at full grasp:

- a) Area goals of 5000 cm² at 8 keV, 10,000 cm² at 2 keV.
- b) Energy band 0.2–10 keV.
- c) Spatial resolution specified at < 30 arcsec.

2. Medium resolution spectroscopy below 3 keV:

- a) Resolving power > 250.
- b) At maximised grasp.

3. High resolution spectroscopy at some energies:

- a) Oxygen-K and Iron-K lines priority.
- b) Resolving power > 1000

Within ESA's long term scientific programme Horizon 2000, a ceiling of 400 MAU at 1985 economic conditions, was set for cornerstone missions of which XMM is the second. This is equal to about US\$ 500 million today. As in all ESA missions, this sum includes spacecraft development, the launch vehicle and orbital operations for two years (though XMM is expected to have a lifetime of 10 years). In the case of XMM it also includes the procurement of X-ray optics, but not the cost of the instruments, which are provided by national funding.

Y. Kondo (ed.), Observatories in Earth Orbit and Beyond, 129–140.

©1990 Kluwer Academic Publishers. Printed in The Netherlands.

TABLE I
XMM mirror module – optical design

Focal length	7500 mm
Mirror radius	159–350 mm
Mirror wall thickness	0.66–1.26 mm
Axial mirror length	600 mm
Minimum packing distance	1 mm
Reflective surface	iridium/gold
Number of mirrors	58
Mirror module mass	170 kg

System level studies carried out in industry and supported by scientific working groups led to the present telescope/instrument concept of XMM as indicated schematically in Figure 1. Three independent telescopes are to be flown each with a CCD camera in the focal plane. On the two telescopes, fixed reflection gratings intercept 50% of the beam to feed strip CCD, secondary focus cameras to provide simultaneous spectroscopic coverage. A practical arrangement within the technical and financial constraints could not be found for a high resolution, dispersive spectrometer. However, in the light of XMM's X-ray sensitivity, a UV/optical telescope to give a simultaneous optical view of the X-ray field is included.

2. System Constraints and Configuration

Experience with the EXOSAT demonstrated the virtues of an X-ray observatory in a highly eccentric orbit (HEO), e.g. the ease of operation and long uninterrupted observing times. Thus while a HEO would be natural for XMM, the choice was further enforced by the aim to use purely passive cooling for CCD's (–100 degC required) as a means to achieve a long-lived mission. Economic considerations led to the selection of the Ariane 4-2L, capable of lifting a 2.4 tonne spacecraft into a 24 hour 70,000 km apogee, 60deg inclination orbit. These orbital parameters permit the use of a single ground station which can view XMM without interruption when it is above 40,000 km, i.e. beyond the background of the radiation belts. Seventeen hours per day (70%) are thus available for observations.

3. X-Ray Optics

Within the overall mass budget, up to 220 kg has been allocated on one mirror module, implying the use of a lightweight replication process for mirror manufacture. The principal characteristics of a mirror module are given in Table I. In the

TABLE II
Characteristics of XMM's prime focus CCDs

	pn CCD	MOS CCD
Number of CCD's/camera	12	8
Depletion Depth (μm)	280	30
Quantum efficiency (%)		
0.5 keV	60	60
1.0 keV	90	90
10.0 keV	90	25
Spatial resolution (μm)	150	20
Spectral resolution (eV)		
0.5 keV	50	50
6.7 keV	130	130
Time resolution mode:		
Full frame transfer (s)	0.024	50
High time (μs)	20	2000
Electron Radiation Tolerance (krad)	1000	14
Operating Temperature (K)	175	175
X-ray CTE (per pixel)	0.99999	0.99998
Background rejection (%)	99.999	99

currently baselined process, each Wolter I shell carrier (paraboloid and hyperboloid in one piece) of CRFP is laid upon a steel mandrel, having a shape tolerance of 10 micron and a surface roughness below 0.25 micron rms. The gold (or iridium) layer is evaporated on to a glass mandrel polished to a surface accuracy of better than 5 \AA . The coated mandrel and the CFRP carrier are moulded together using a 50 micron epoxy layer and after curing the shell is removed from the mandrel.

In the technology development programme three mirror modules have been produced in this way and tested at the Panter facility in Munich. With 'full beam' illumination, half energy widths of 67, 70 and 94 arcseconds have been achieved at 0.93, 1.49 and 8.05 keV respectively. Pencil beam measurements along a meridian showed a best resolution of 11 arcsec (HEW) with 22 arcsec (HEW) average. This indicates some global deformation of the carrier during the replication/demoulding process.

The nickel electro-forming process is also being pursued, which has demonstrated good performance in the SAX double cone approximation and JET-X programmes. The main difficulty with this process for XMM is of course the mass limitation. However, it is faster and less expensive than CFRP replication.

The decision in mirror technology should be taken in April 1991. A mirror development model containing three of the 58 shells produced to full X-ray standard, together with the 'electro-optical' models of the instruments are scheduled for testing in the Panter facility in October 1992.

The effective area of the XMM optics as a function of energy and comparisons with other missions shown in Figure 2, while the off-axis performance is shown in Figure 3.

TABLE III
 Characteristics of XMMs reflection grating spectrometers

Spectrometer readout		MOS CCD's
Number of CCDs/readout camera		10
Grating mean line density (1/mm)		641
Grating configuration		In-Plane
Number of grating plates/module		240
Grating technology		Beryllium/replication
Waveband (Å)		
	Order = - 1	5-35
	- 2	5-20
	- 3	5-10
Maximum resolving power	5 Å	200
	10 Å	360
	15 Å	500
	25 Å	430
	35 Å	560

CCD Prime Focus Camera's - PI G. Bignami.

A number of options for the CCD devices are currently under investigation, including the pn CCD and the MOS CCD (see Figure 2, 4 and 5 for characteristics).

Reflection Grating Spectrometer - PI A.C. Brinkman

The characteristics of this instrument are shown in Table III and in Figure 4.

Optical Monitor - PI K.O. Mason

This 30 cm aperture Cassegrain telescope will span the UV/Optical range from 1500 to 10,000 Å using two detectors, a microchannel plate for the 'blue' beam and a CCD for the 'red' beam. The latter will cover the same FOV as the X-ray telescopes. Characteristics are shown in Figure 4.

4. Sensitivity

The sensitivity of XMM is crucially dependant on the collecting area of the X-ray optics (58 shells per telescope), the achieved angular resolution (< 30 arcsec) and the quantum efficiency and energy range coverage of the CCD's. Assuming nominal performance, then the minimum detectable source strength as a function of time as in Figure 6 should be obtained. In one XMM orbit of 60,000 sec the minimum detectable source would be approaching 10^{-15} erg cm^{-2} s^{-1} . For every typical exposure of 10^4 sec a limiting sensitivity some 20 times fainter than the Einstein Deep Survey will be achieved.

The minimum detectable line strength is indicated in Figure 7. For a full orbit's observing an Oxygen line with an equivalent width of 90 and 200 eV will be detected from a source with a flux of 10^{-14} erg cm^{-2} s^{-1} by the cameras and reflection gratings respectively.

TABLE IV
Characteristics of XMMs optical monitor

Telescope Type	Cassegrain	
Primary mirror diameter (mm)	30	
Characteristics	Blue Beam	Red Beam
Angular field (arcmin)	8	30
Plate scale ($\mu\text{m}/\text{arcsec}$)	37	6
Spatial resolution (arcsec)	1	4
Detector	MCP	CCD
Spectral range (\AA)	1500-6500	4000-10000
Magnitude limit in 1000 s	24.5	21
Magnitude of brightest star	14.5	6 (in 0.25 s)

5. XMM As An Observatory

Figure 8 shows the allocation of guaranteed observing time granted to PIs, mission scientists and the observatory team and open time for the general observer. The first year of observations is largely taken up by guaranteed time but by the second year, 75% of the time is open. For the third and subsequent years, all observing time will be open to general observers.

References

Peacock, A., Taylor, B.G., Ellwood, J.: 1990, *Adv. in Space Res.* **10-2**, 273-285

XMM – OPTICAL PATH DIAGRAM

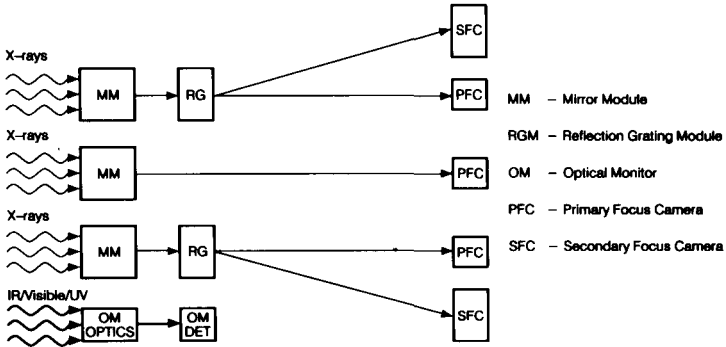
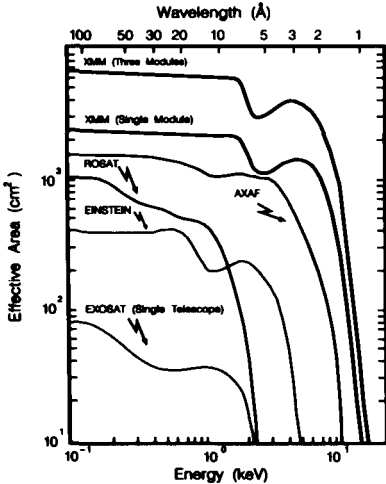


Fig. 1. Schematic of XMM's instruments.

XMM MM PERFORMANCE CHARACTERISTICS

Effective Area:

Resolution:



Requirement < 30 arc sec HEW (TBV)

Fig. 2. Effective area of the XMM X-ray optics as a function of photon energy compared with other missions.

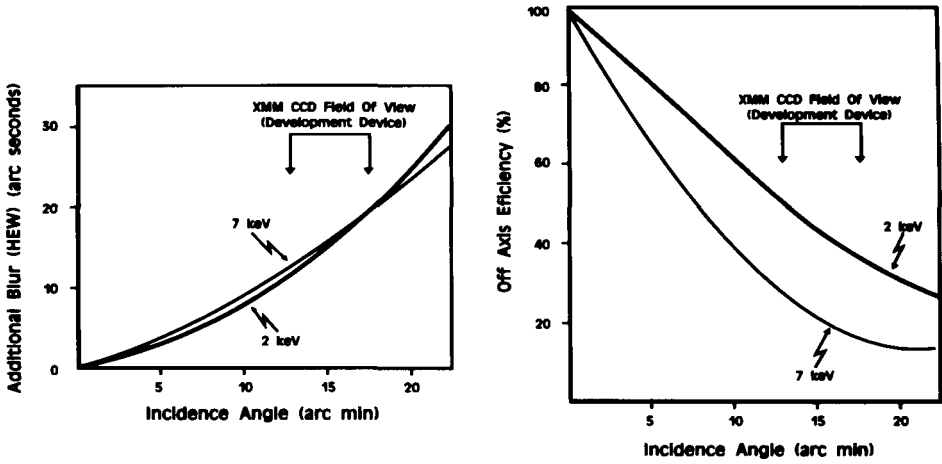


Fig. 3. Variation in the additional blur contribution to the spatial resolution and off-axis telescope efficiency for two X-ray photon energies as a function of angle of incidence.

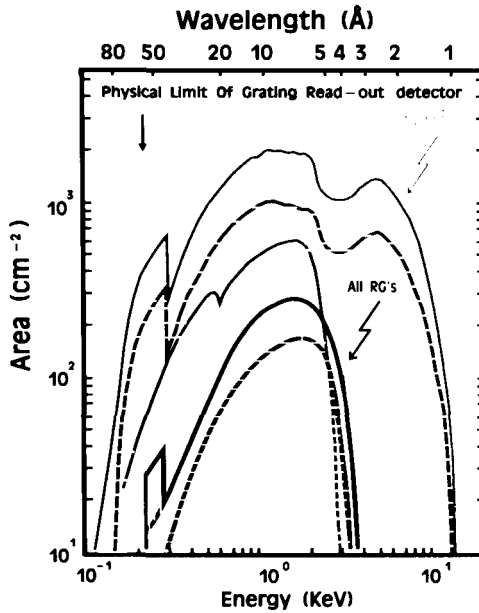


Fig. 4. Effective on-axis area of the XMM CCD camera fitted to all three telescope modules (upper curves) and to a single module (dashed curve). Note that the effect of the loss of area due to the reflection gratings behind two telescopes has been included in the total area (full curve). The effective area of the gratings is also shown.

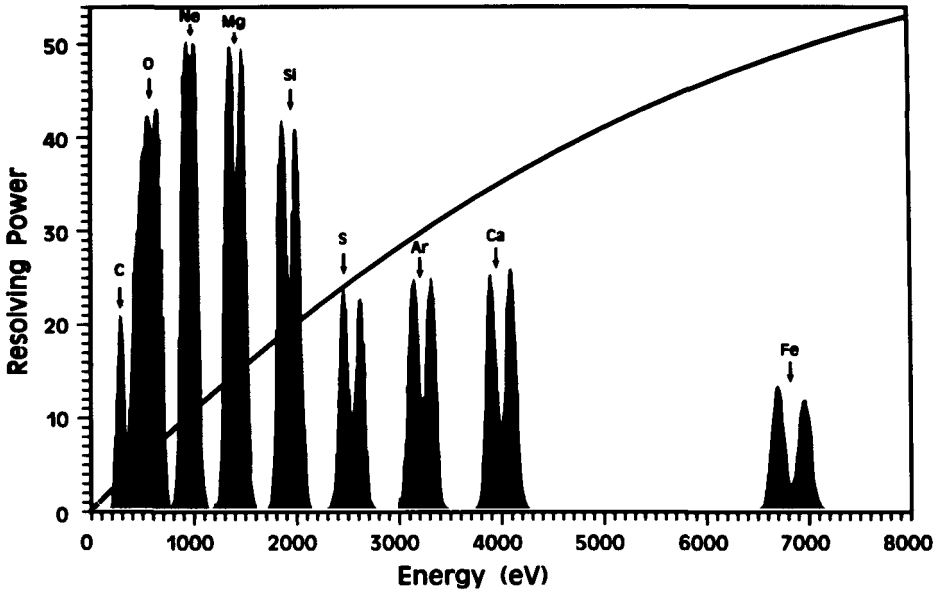


Fig. 5. Resolving power of the XMM CCD as a function of photon energy. The CCD and mirror responses have been combined and all transitions set at equal strength.

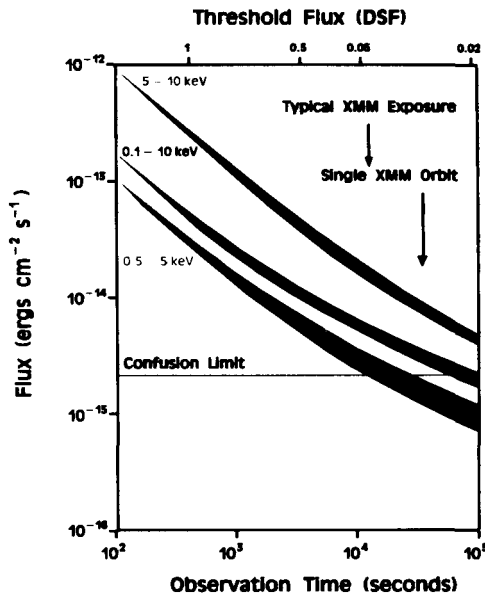


Fig. 6. Minimum detectable source strength as a function of observing time. The equivalent threshold flux in units of the Einstein Deep Survey (DSF) is indicated.

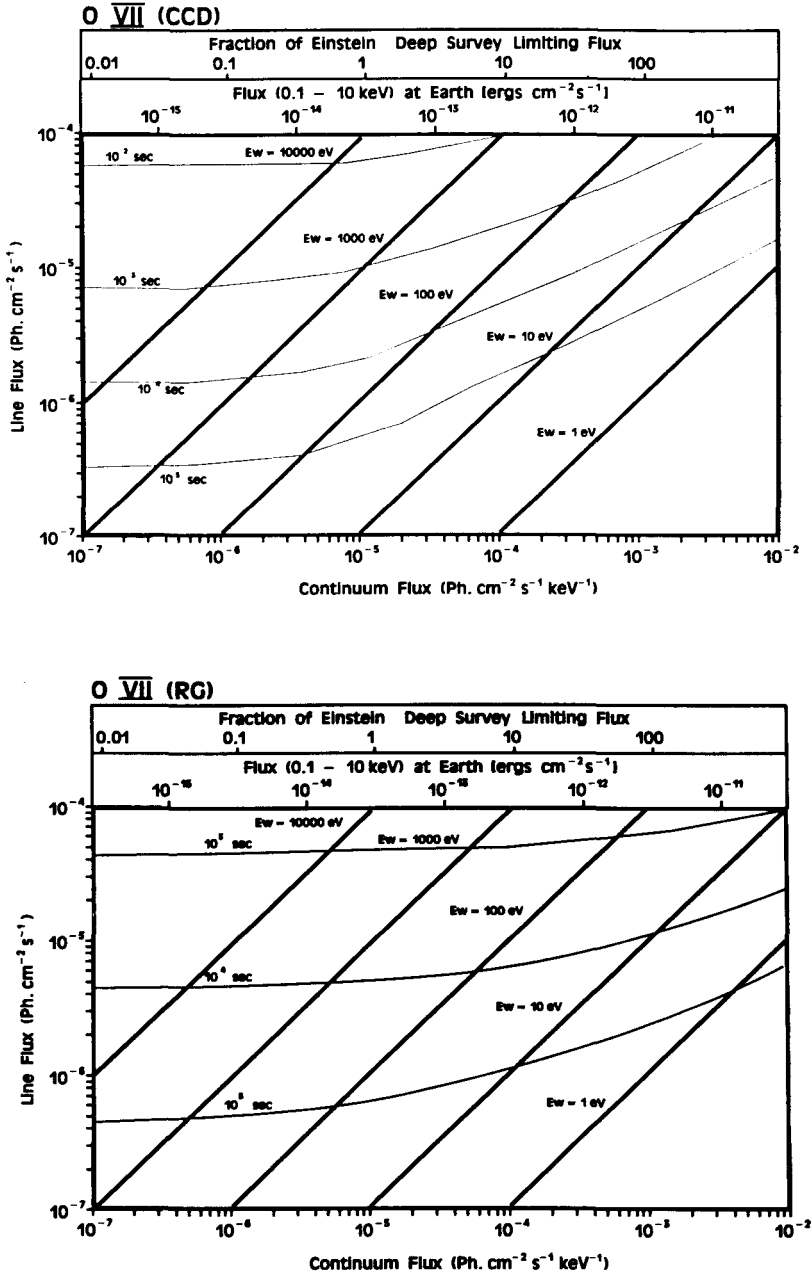


Fig. 7. (a)–(c). Minimum detectable line strength as a function of continuum flux at the He-like line energies of O (a), Si (b) and Fe (c), for both the CCD and grating modules.

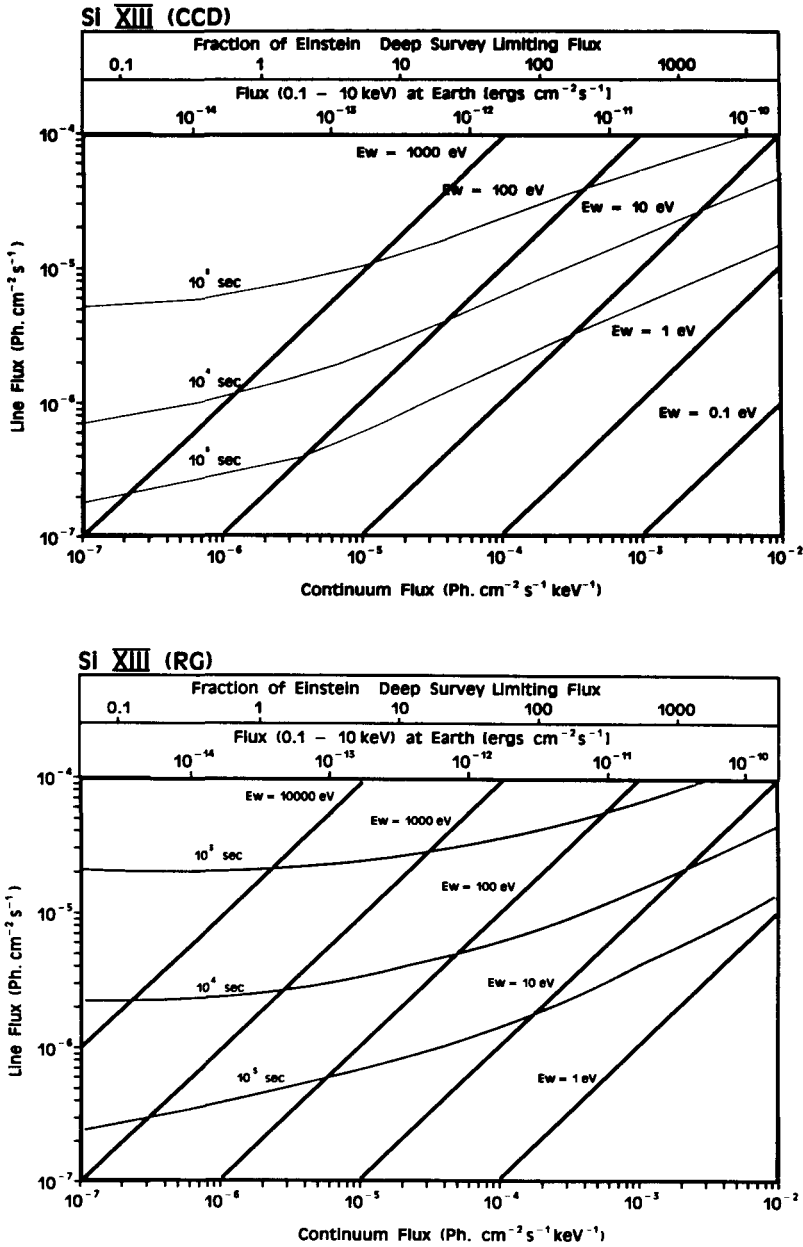


Fig. 7b.

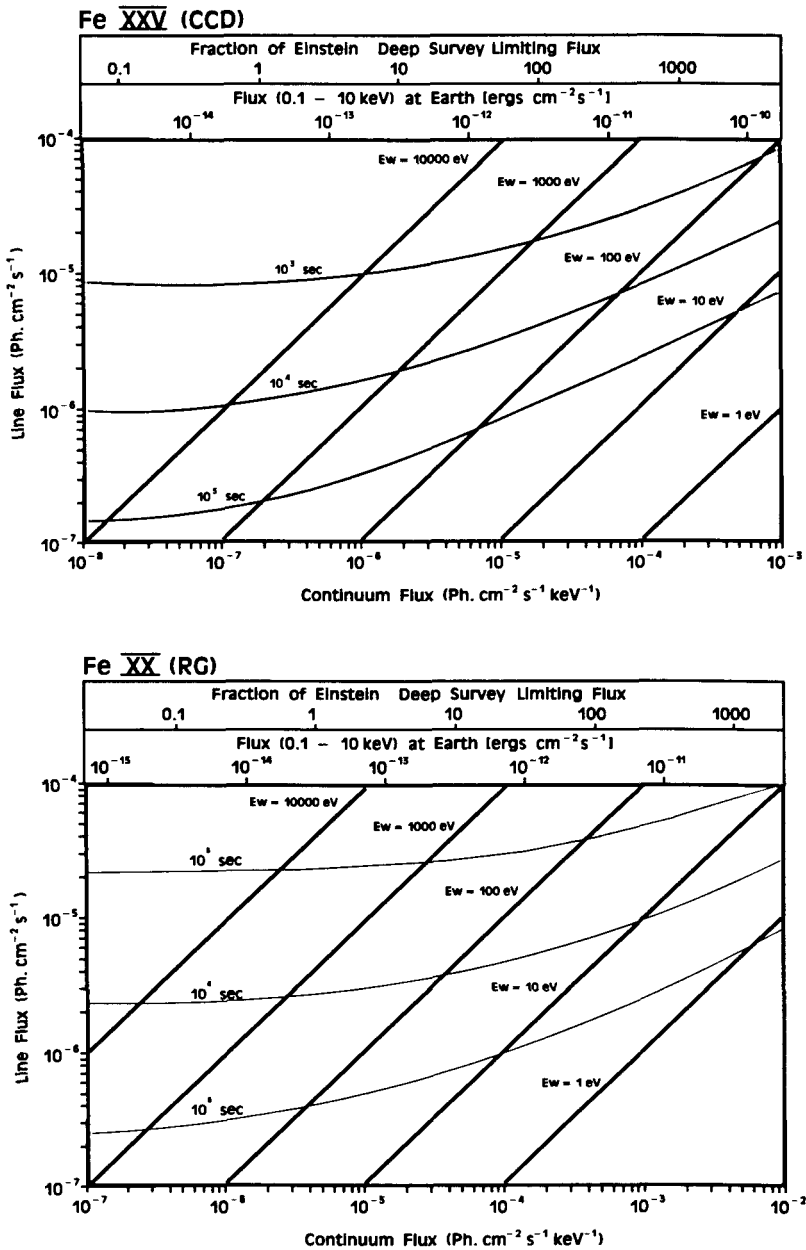


Fig. 7c.

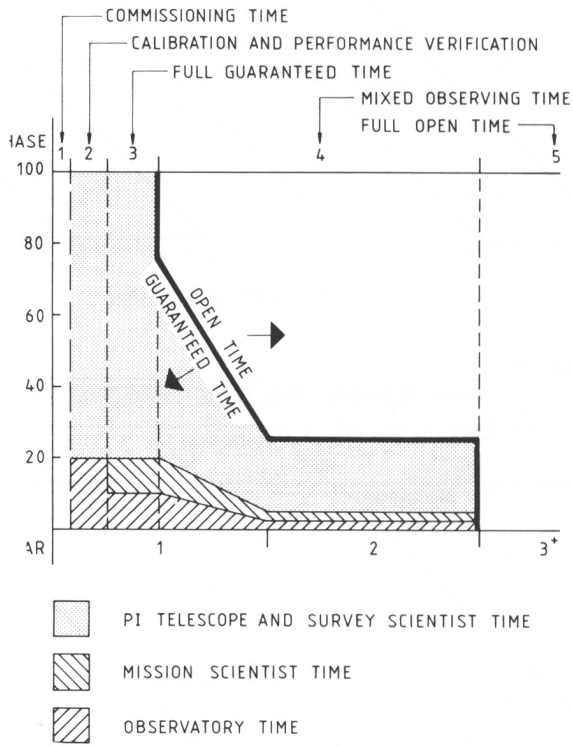


Fig. 8. The allocation of XMM observing time.